

INTERNATIONAL SOCIETY FOR SOIL MECHANICS AND GEOTECHNICAL ENGINEERING



This paper was downloaded from the Online Library of the International Society for Soil Mechanics and Geotechnical Engineering (ISSMGE). The library is available here:

<https://www.issmge.org/publications/online-library>

This is an open-access database that archives thousands of papers published under the Auspices of the ISSMGE and maintained by the Innovation and Development Committee of ISSMGE.

Geotechnical studies and design of La Yesca Dam

J.D. Alemán Velásquez, A. Pantoja Sánchez & S. Villegas Lesso
Comisión Federal de Electricidad, GEIC, México



ABSTRACT

The hydroelectric project La Yesca is currently under construction in the state of Jalisco, Mexico. The concrete face rockfill dam (CFRD) will be 205 m in height, one of the highest in its type. This article describes the general characteristics of the project and some of the field and lab works, as well as the studies and analysis performed to carry out the geotechnical design of the structure.

RESUMEN

El proyecto hidroeléctrico La Yesca está actualmente en construcción en el estado de Jalisco, México. La cortina de enrocamiento con cara de concreto (CFRD) tendrá una altura de 205 m y será una de las más altas en su tipo. Este artículo describe las características generales del proyecto y algunos de los trabajos de campo y laboratorio, así como estudios y análisis realizados para el diseño geotécnico de la estructura.

1 INTRODUCTION

La Yesca hydroelectric project is located on the Santiago river, 105 km NW of the city of Guadalajara and 22 km NW of the small town of Hostotipaquillo in the state of Jalisco, Mexico. The Santiago riverbed is the legal state line between Nayarit and Jalisco. The damsite is located 4 km downstream of the confluence of the Bolaños and Santiago Rivers, upstream of El Cajón and downstream Santa Rosa hydroelectric power plants (Fig. 1).

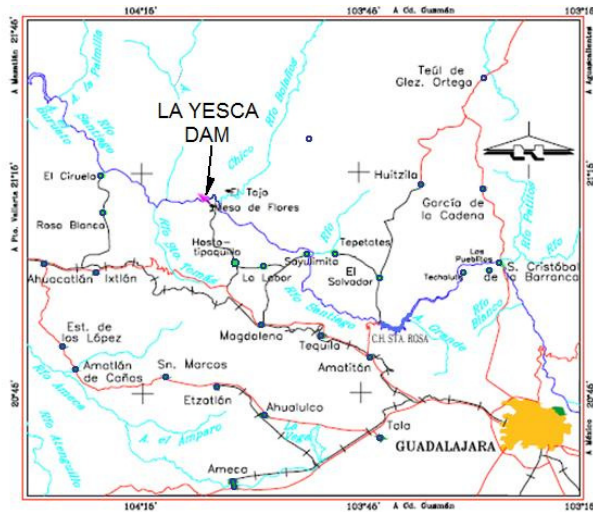


Figure 1. La Yesca hydroelectric project location.

This project considers a power plant equipped with two vertical Francis turbo generators of 375 MW each, allowing a total annual average generation of 1 210 GWh with a plant factor of 0.19. The reservoir will also help regulate the river runoff from its own basin and contribute to optimize the electric generation at El Cajón power plant.

In the first part of this article, a brief description of the site's geological conditions and of the main project structures is presented. The second part details the work done for the geotechnical design of the dam.

2 PROJECT DESCRIPTION

The general layout of La Yesca hydroelectric project is presented in Fig. 2.

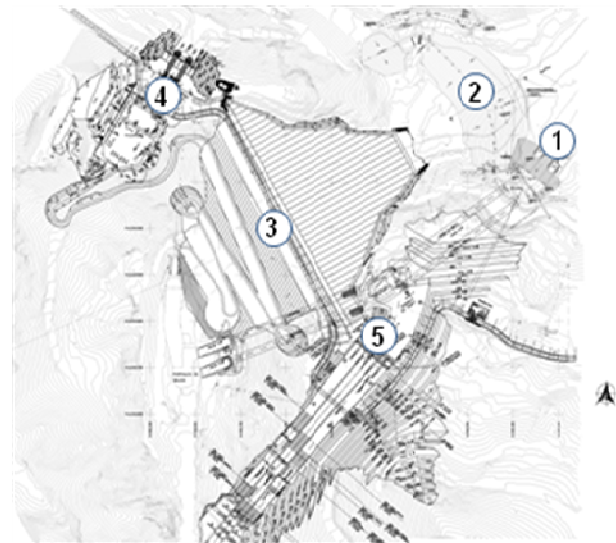


Figure 2 General layout of the project: 1, Diversion tunnels, 2, Cofferdam, 3, Dam, 4, Underground powerhouse, 5, Open channel spillway.

2.1 General Geology

The canyon of La Yesca damsite was carved by the Santiago River on a group of Cenozoic volcanic rocks,

oceanic plates under the continental plate; the activity of the Trans Mexican Volcanic Axis; and the seismic active area of San Cristobal de la Barranca, Jalisco, in which a 7.3 °R earthquake took place (Malagon, 1989). From the point of view of seismic generation, the first and third sources of earthquakes appear to make the dominant contribution. The parameters for the Operating Basis Earthquake (OBE) and for the Maximum Design Earthquake (MDE) are: $a_o = 0.14$ g and 0.41 g; $c = 0.38$ g and 1.02 g, respectively (Fernández R S, 2006). With these parameters, dynamic analyses were made and the result for the Maximum Credible Earthquake (MCE) is an embankment total settlement of less than 60 cm.

3.2 Field works

3.2.1 Alluvial and rockfill test embankments

For the first stage, a gravel-sand test embankment was built up to a height of 10 m (see Fig.4). Three areas were managed with different layer thickness (0.6 m, 0.8 m and 1.0 m). The layers were compacted with a 12.2 ton of static weight vibrating drum roller by varying the number of passes and determining the void ratio every two passes.

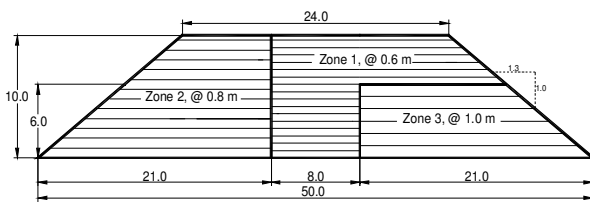


Figure 4. Section of the alluvial test embankment.

For the second stage, a 10 m high rockfill test embankment was built, three areas were also used with different layer thickness (0.8 m, 1.0 m and 1.2 m) and compacted by using the same 12.2 ton of static weight vibrating drum roller.

The rockfill test embankment was built by adding 200 L/m³ of water before compaction of each layer. It was observed that the addition of water improved significantly the compactness of the rockfill embankment. The gravel and sand embankment was compacted practically dry, after realizing that the addition of water did not improve its mechanical properties.

The embankments were instrumented with floating type reference plates to get the settlements in selected points. Additionally, the settlement of each layer surface was measured by accurate surveying, in a grid of 6.0 x 4.5 m points, every two passes of the drum roller.

Also, volumetric samplings were made every two passes of the drum roller, in order to measure the variation of the void ratio with the number of roller passes, as well as the grain sizes, dry density and consistency limits in the materials obtained in each and

every one of the samplings. In addition, confined plate tests and Matsuo-Akai type permeability tests were done.

The results of these tests are summarized in the following tables and figures.

Table 1. Void ratio variation in the gravel-sand test embankment.

Layer Thickness m	Void ratio		
	Number of passes		
	4	6	8
0.60	0.258	0.247	0.233
0.80	0.250	0.25	0.239
1.0	--	0.257	0.292

Table 2. Void ratio variation in the rockfill test embankment.

Layer Thickness m	Void ratio*	
	Fluidal Dacite	Porphyritic dacite
0.80	0.336	0.361
1.0	0.331	0.410
1.2	0.368	0.422

* For 8 passes of 12.2 tons compactor roller

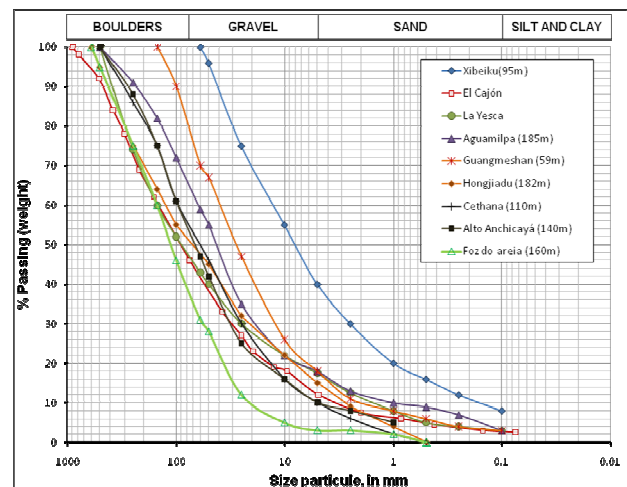


Figure 5. Average grain size distribution curves used in 3B zone of several dams.

3.2.2 Permeability

Fifteen Matsuo-Akai type permeability tests were made in the alluvial test embankment and eleven in the rockfill embankment. An average permeability coefficient (k) value of 1×10^{-1} cm/s was obtained for the first one, while in the second one, all tests yielded values of k greater than 1 cm /s.

3.2.3 Deformability

The deformability measurement of the materials in the test embankments was done in two ways: through plate tests and through the instrumentation results.

The plate tests were strongly influenced by scale effects and the influence of the poor containment, especially in the alluvial test embankment, so their results were not taken into account.

On the other hand, the results obtained from the instrumentation (measuring the settlement of the test embankments due to its own weight), gave more reliable values.

The settlement of the test embankment is produced by a load increase due to the increase of embankment height and is calculated on the difference between the height of the anchor in the body of the test embankment and the elevation of the top of the bar.

After measuring the settlements of the test embankments with the bar extensometers and obtaining the volumetric weights from the samples obtained, it is possible to determine the deformability modules of the material from every zone that constitutes the test embankment, considering the thickness of the layers of the material, by using the following expression (Hernández R. et al 2006):

$$E = \left(\frac{\sigma \cdot H}{\delta} \right) v_c$$

Where:

E = Deformability module, in MPa

σ = Geostatic stress in the extensometer location, MPa

H = Thickness of the layer under the extensometer, in meters.

δ = Settlement measured in the extensometer, m

v_c = Theoretical relationship between free and confined modulus. Typically has a value of 0.74 for a Poisson ratio of 0.3 (measured in earth and rockfill dams).

The average results of deformability of the modules in each layer are shown in table 3:

Average deformability modulus for materials used in the test embankments.

Layer Thickness m	Average deformability modulus E , in MPa		
	Gravel	Rockfill ¹	Rockfill ²
0.60	277		
0.80	256	148	174
1.00	246	135	158
1.20		126	150

1: Fluidal dacite rockfill

2: Porphyritic dacite rockfill

3.3 Laboratory tests

3.3.1 Index tests

Some of the results of tests done on the construction materials are listed in the table 4.

The failure load values obtained from the grain rupture test, appear in the table 5, where values of El Cajon dam materials have also been included as a reference.

Table 4. Values of several index properties.

Test	Material		
	Gravel	Rockfill ¹	Rockfill ²
Absorption	< 2.25%	<2.2%	<2.3%
Accelerated weathering	< 1%	<9%	<5.3%
Abrasion (Los Angeles)	<12.5%	<14%	<17%

1: Fluidal dacite rockfill

2: Porphyritic dacite rockfill

Table 5. Grain rupture load (Pa) results

Material	Rupture Load, in kN	
	Dry	Saturated
Gravel La Yesca	12	10
Fluidal dacite La Yesca	5	3.5
Porphyritic dacite La Yesca	4.8	4
Ignimbrite El Cajón	1.9 to 3.3	1.7 to 2.6

Compression strength of 5 cm diameter grains on the average

These results, that involve the influence of the form and the hardness of the grain in the deformability parameters, confirm that the alluvium is much less deformable than the rockfill embankment, which is consistent with both the experience observed in other dams and the parameter values measured in the test embankments.

3.3.2 Shear strength and deformability in giant triaxial tests

Consolidated drained (CD) triaxial tests were done in giant rockfill test samples of 30 cm in diameter and 70 cm high. The results are shown in figures 6 and 7. The tests were executed on samples with a maximum grain size of 38mm, coefficient of uniformity similar to site one, and the void ratio in the range of 0.30.

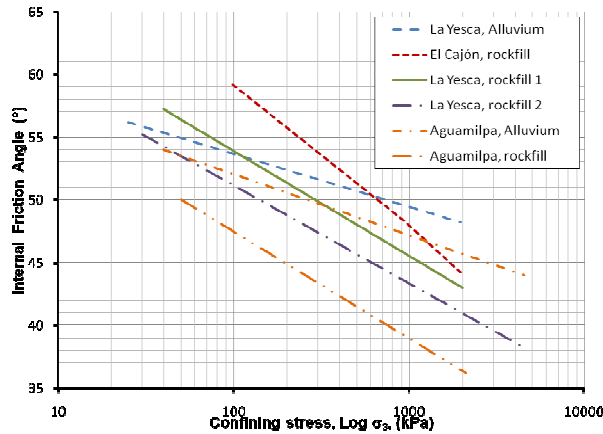


Figure 6. Effect of the confinement stress on the friction angle.

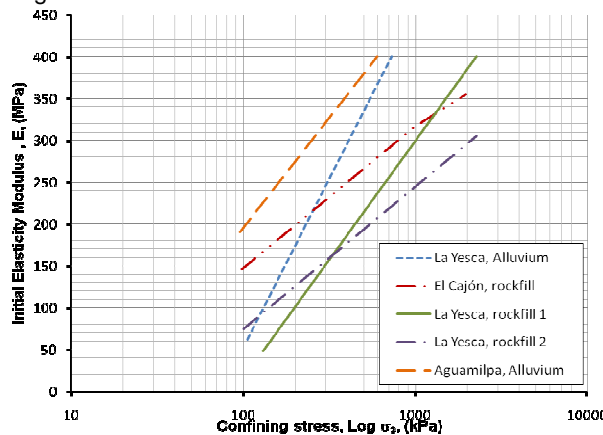
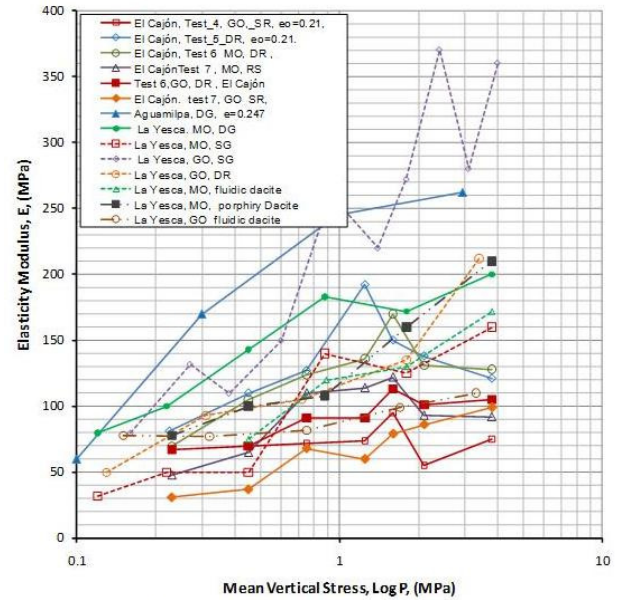


Figure 7. Confinement stress effect on initial tangent deformability modulus (E_i)

3.3.3 Deformability in Odometer

The figure 8 groups the results of variation in elastic modulus obtained from tests with rockfill in mid size odometer (samples of 30 cm in diameter and maximum particle size of 3.8 cm), and tests with giant odometer (samples of 110 cm in diameter and maximum particle size of 17 cm). Tests were carried out in both dry and saturated conditions.

In general, La Yesca rockfill deformability is smaller than the ignimbrite rockfill one at El Cajon dam, while the alluvium showed a very low deformability, similar to Aguamilpa dam sand and gravel 2B material.



Symbology:

MO, Medium odometer, 30 cm diameter
 GO, Giant odometer, 113 cm diameter
 DR, Dry rockfill
 DG, Dry gravel
 SG, Saturated gravel
 SR, saturated rockfill

Figure 8. Elastic modulus obtained in odometer tests.

4 ANALYSES AND DESIGN

4.1 Overview

La Yesca dam will be the highest of its kind in America and one of the highest in the world. Recently some high dams of this kind have endure strong cracking in the concrete face, which in turn has led to large leaks of the order of several cubic meters per second.

It appears that the origin of these cracks are the high deformability of the embankment rockfill placed in those dams, so in order to avoid these effects in La Yesca dam, special emphasis was put on the strain-stress analyses to calculate the possible movements of the concrete face and the compressive stress induced on the slabs due, to the embankment deformation. In this way we could define the most adequate construction specifications.

Therefore, the zoning design of La Yesca dam was made to meet the following criteria:

- Achieve low deformability of the 3B zone in the rockfill embankment
- Get a transition zone between the 3B zone material and the 3C zone rockfill at the embankment.
- Keep the deformability modulus ratio among adjacent zones in the embankment less than 2.
- Attain effectiveness and efficiency of construction materials this is, proper behavior at a reasonable cost.

It was also considered that the perimetric and tension joints will have barriers against leakage similar to those used in El Cajon dam (copper seal both in the lower and upper face of the joint as well as self-sealing material covering them), installed strictly following the corresponding specifications.

4.2 Upstream and downstream slopes

The upstream and downstream slopes of this type of a dam are generally steeper than the core zoned earth and rockfill dams because the embankment is not submerged thus there is not reduction of the shear stress for submergence in both the static and dynamic loading. With good quality rockfill, in low or medium

seismicity, 1.4:1 slopes are generally good enough to get the proper safety factors needed, when materials of relatively low shear strength are used, the slopes are downsized to 1.5:1 or less, depending on the stability analyses results.

Initially the slopes considered for La Yesca dam were 1.5:1 for the upstream and 1.48:1 for the downstream slopes, based on the Aguamilpa dam experience. After performing the slope stability analyses, it was feasible to have 1.4:1 for both upstream and downstream slopes.

The main cross section of the dam considered for analysis is shown in figure 9. The grain size bands specified for the building materials are presented in figure 21 and in table 6.

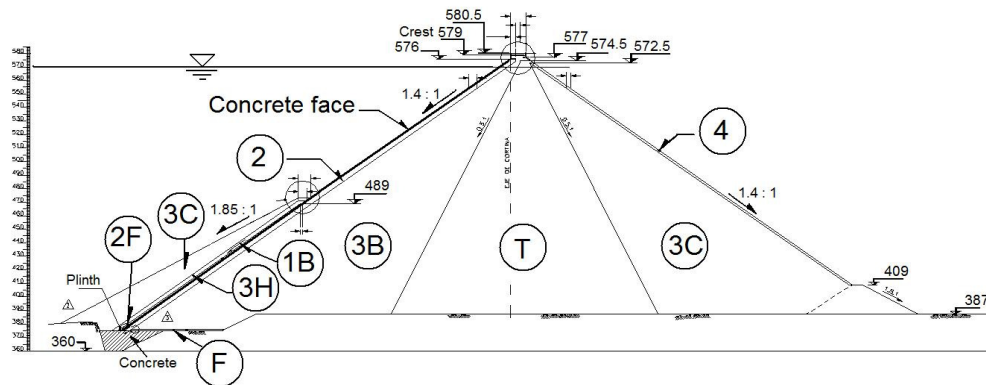


Figure 9. Maximum cross section of La Yesca dam, showing material zoning.

4.3 Displacements and deformations analysis

E_c , Construction deformability modulus.

4.3.1 Deformation modulus required

Accepting a maximum displacement of the concrete face in the order of 20 cm (The greatest displacement of El Cajon dam was about 22 cm, with top seepage values of 160 L / s, while Aguamilpa dam maximum displacement is in the order of 12 cm, with minimum seepage values) and using the equation (Hacelas, 1999), we have:

$$E_{II} = 0.003 H^2 / \delta \quad (3)$$

Where:

E_{II} , Deformation modulus of material 3B used in the filling, in MPa

H , Height of the dam, in m.

δ Maximum displacement of the concrete face, in m.

And considering a relation $E_{II}/E_c = 2$ (value usually found in practice) we have:

$$E_c = 0,003 * 204^2 / (2 * 0,2) = 312 \text{ MPa}$$

Where:

Under these conditions a main rockfill embankment (3B) with a deformability modulus in the order of 300 MPa is required. This value is only obtainable by using alluvium materials in zone 3B.

4.4 Material properties for numerical analyses

Based on the above information, finite element analyses were carried out to assess the magnitude of the settlements in the dam. PLAXIS V8 software was used for the 2D analyses and FLAC3D 2.10 software for the 3D analyses. The deformability modulus values were defined according to the following criteria:

The deformability modulus of a rockfill or gravel-sand embankments depends mainly on the following factors:

- Hardness and shape of grains (measured by the Grain Rupture Load, in kN).
- Compactness or degree of arrangement achieved (measured by the Void Ratio).
- Grain size distribution (Measured by the Coefficient of Uniformity, $C_u = d_{60}/d_{10}$).
- Maximum Particle Size.
- Wetting of the rockfill before compacting.
- Weight of roller used in compaction, layer thickness and the number of passes.

In general, the deformation modulus, E_c , value increases when the grain rupture load of the materials and the coefficient of uniformity gets larger and both the relation of void ratio and the maximum particle size decreases.

Figure 10 shows a graph that contains the total population of deformability modulus calculated with the different field and laboratory tests for the alluvial and rockfill test embankments (Pantoja, 2006 y 2007), as well as the exponential trend line for alluvial, fluidal and porphyritic dacite materials. Additionally, the vertical, horizontal and estimated octahedral stresses were calculated for dam materials 3B, T and 3C, by using FLAC 3D software at one third of its total height. With these stresses and by using the corresponding trend line graph, the corresponding deformability modulus to perform the 2D and 3D the finite element analyses of the dam were determined. Table 6 presents a summary of index and mechanical properties expected for materials 3B, T and 3C.

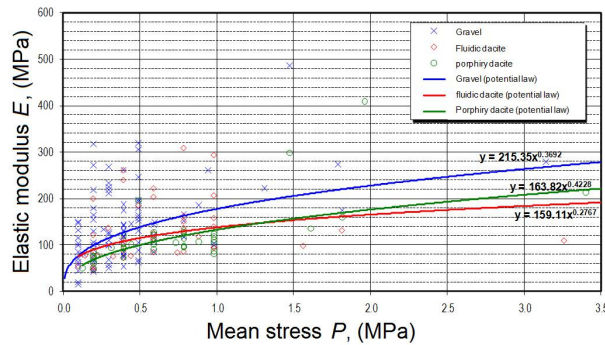


Figure 10. Total population deformation moduli obtained in the studies, and trend lines

Table 6. Parameters used in La Yesca analyses

Material		Volumetric Weight	Poisson ratio	E_c	E_{II}
		kN/m ³		MPa	MPa
3B, Gravel	1*	20.7	0.2	171	226
	2*			240	480
	3*			171	342
T, Rockfill	1*	19.5	0.2	153	169
	2*			130	260
	3*			115	230
3C, Rockfill	1*	18.5	0.25	119	129
	2*			85	170
	3*			85	170

* Parameters used in the analysis: 1, Trend line; 2, Most probable behavior considering Aguamilpa and El Cajon dams experience; 3, Conservative viewpoint

4.5 Analysis of stress and deformations in two dimensions (2D)

Analyses were performed with the finite element method (FEM) in two dimensions using the program PLAXIS V8.0. The materials were modeled with an elastoplastic behavior with a Mohr-Coulomb resistance law. The properties used in the model are indicated in Table 5, based on the geometry and materials zoning of Figure 9.

Here it is worth commenting that, although it is known that, in general, the deformation modulus increases with the degree of confinement (according to the equation: $E_f = E_o (\sigma_c / Pa)^\alpha$, where E_o is the module for $\sigma_c = Pa$, and σ_c is the confinement stress. Usually Pa is taken as 100 kPa), however, performed analysis of rockfill dams built in Mexico have shown that it is possible to model the dam using an elastic linear model, provided that a representative module is selected.

Therefore, the static finite element analysis results are presented in what follows, using a model of this type.

The finite element mesh used for the analysis at the end of construction and filling is shown in Figure 11.

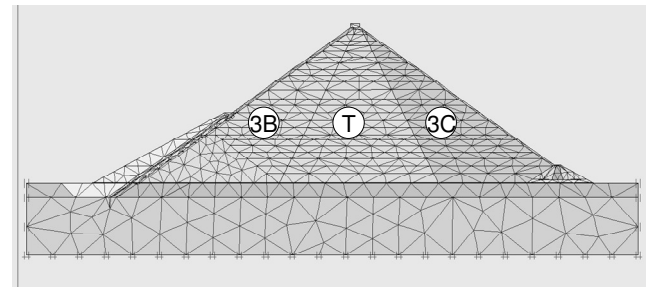


Figure 11. Finite element mesh used for 2D analyses.

The horizontal borders of the 20 steps considered in the construction of the dam are shown. At the end of each stage, a correction of displacements was done to adequately model the accumulated displacements at the end of construction, as the final displacement of the surface at each stage is zero.

Although several cases were analyzed using diverse deformability parameters, the case 2 in the previous table 6 corresponds to the most representative of the future behavior of the dam and will be discussed here follows.

4.5.1 Behavior of the dam at the end of construction

The acting forces in the dam are the body forces, defined by the volumetric weight of the materials and their distribution.

The maximum vertical settlement in the center of the curtain was 0.93 m. The horizontal displacement, in the 3B and 3C material zones was 0.48 m. The total horizontal displacement in the center of the curtain was 0.94 m.

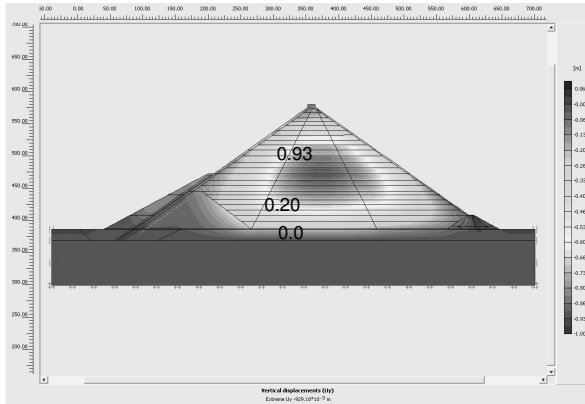


Figure 12. Vertical displacement contours at the end of construction.

4.5.2 Behavior of the curtain and the concrete face with the reservoir filling

The maximum vertical calculated settlement of the concrete face was 0.13 m and the horizontal displacement of 0.34 m. Both at an elevation 475.00, approximately. The total displacement of the curtain was of 0.35 m.

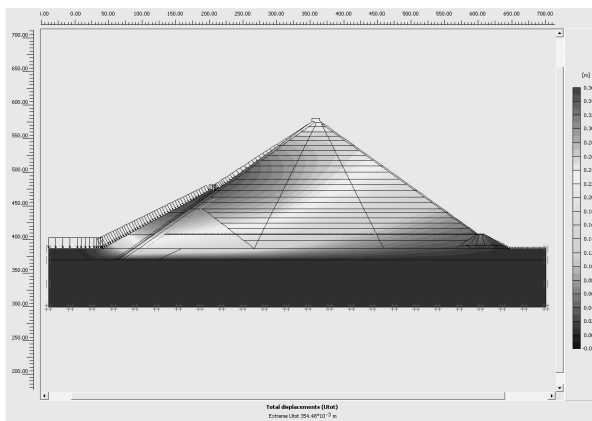


Figure 13. Total displacements contours due to filling.

4.6 Analysis of stress and strains in three dimensions (3D)

The numerical analysis was performed using the FLAC3D (Itasca Consulting Group), which allows to run three dimensional numerical modeling of advanced geotechnical problems. Basically the capabilities FLAC3D were used to model two aspects: a) The process of building the dam, which must be modeled as a layer sequence, and b) The first filling of the reservoir, applying the hydrostatic loading of the water on the concrete face.

In this analysis, the elastic linear model was considered as the constitutive model for earth materials, due to the excellent concordance observed between the measured and calculated by using this model in other dams built in Mexico.

The three dimensional model of the curtain for the construction sequence is shown in Fig. 14. During construction of the model, the shape of the dam and its contact with the walls of the canyon, was reproduced as close as possible.

The results presented below are in terms of displacements contours and stress of the curtain and concrete face.

In the analysis of the first filling of the reservoir, the slab embankment contact was modeled considering that there would be no relative displacements between them. This is a simplified approach, which is not far from reality, because the high shear resistance generated for the range of normal stresses that occur in a slab-embankment contact, virtually preventing the occurrence of a failure in this interface.

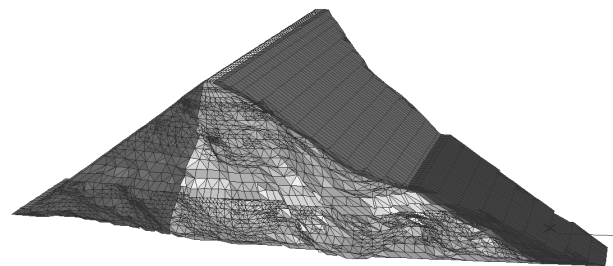


Figure 14. 3D finite element mesh used in the analyses

In the analysis presented in this report, the existing vertical joints in the concrete face were not included, resulting in extreme conditions in some aspects, such as, the horizontal tension stress in the lateral side of the concrete face and in the joints. In spite of this, based on the experience with other dams (Alemán JD, et al 2005, 2007) the results obtained define quite precisely the zones of compression and tension on the concrete face as well as the order of magnitude of these values.

A linear elastic model for the materials of the dam and the concrete face was used, taking into account, the differences that arise between the vertical module used during construction and the module used during the filling.

4.6.1 Dam behavior at the end of construction

The vertical and horizontal stresses generated within the dam at the end of construction, for materials 3B, T and 3C, were 0.3, 0.4 and 0.3 MPa, respectively as first results. The maximum vertical stress in the Zone T was in the order of 3.5 MPa.

The maximum vertical settlement in the embankment was of 0.80 m, approximately in the center of a longitudinal section. The maximum vertical settlement in a cross-section of the dam was of 0.81 m.

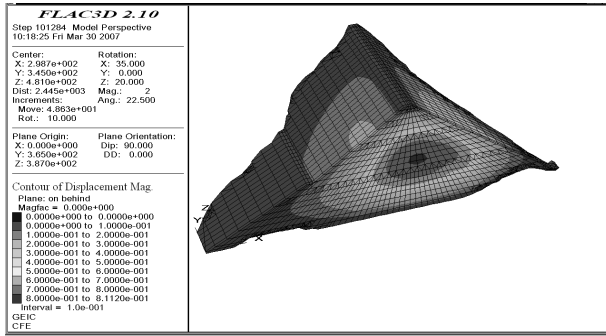


Figure 15. Total displacements contours at the end of construction.

The maximum horizontal displacement was variable between 0.04 m in the area of material 3B (upstream) and 0.11 in the 3C material (downstream).

The maximum total displacement, in a cross section, was of 0.81 m in the center of the dam.

4.6.2 Embankment and concrete face behavior with the reservoir filling

The maximum Mag vertical settlement in a cross section of the dam was of 0.124 m in the upstream slope. The maximum horizontal displacement along the axis of the river was 0.14 m in the upstream slope, both values at elevation 475 m.

The maximum total displacement of the concrete face was of 0.17 m, approximately, in the center of its height and length.

The maximum horizontal displacement in the concrete face, in the dam axis was of 0.03 m.

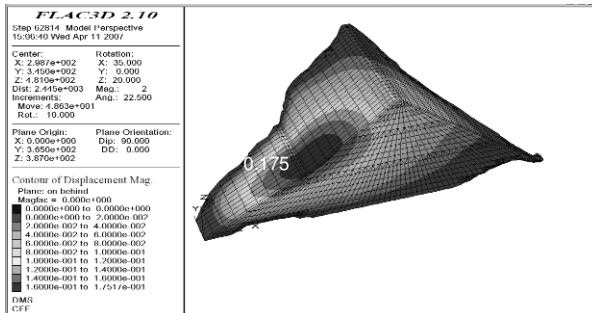


Figure 16. Total displacement contours due to reservoir filling (in m)

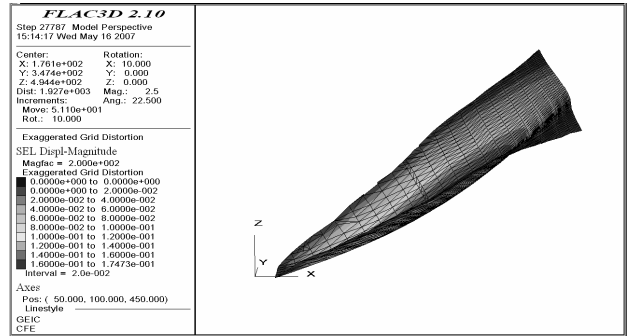


Figure 17. Deformation of the concrete face due to reservoir filling.

The compression and horizontal stresses generated in the concrete slabs due to the filling of the dam, were of 4.8 MPa or below, and were located in the center of the slab. The maximum tension stress was 9.8 MPa and occurred in small concentrated areas located in the contact edges of the slab with the abutments (Figures 18 and 19). Taking into account the average maximum stress in the area near the abutments, the maximum average tensile strength is of 3 MPa.

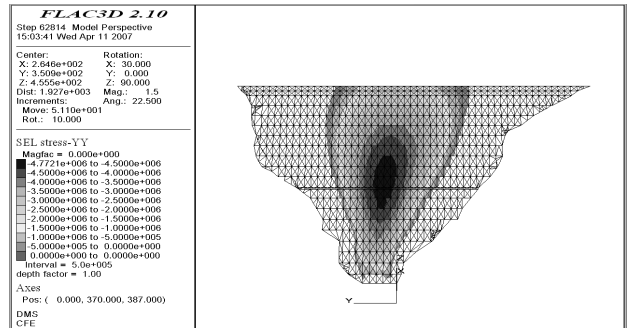


Figure 18. Horizontal compression stress in the concrete face (kPa).

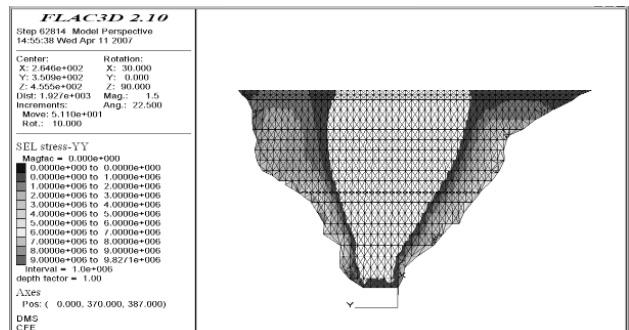


Figure 19. Horizontal tension stress in the concrete face, kPa.

The stresses generated in the slabs due to the filling of the reservoir in the direction of the dam slope were

calculated obtaining a maximum compression value of 1.43 MPa in the center of the height and length, and a maximum tension stress of 5.47 MPa located in small concentrated areas near the contact edges of the slabs with both abutments. Taking into account the average maximum stress in the area near the abutments, the tensile stress is of 2.5 MPa.

The horizontal compression stress and tension zones of the concrete face, where the construction joints are located, were defined with this information and can be observed in figure 20.

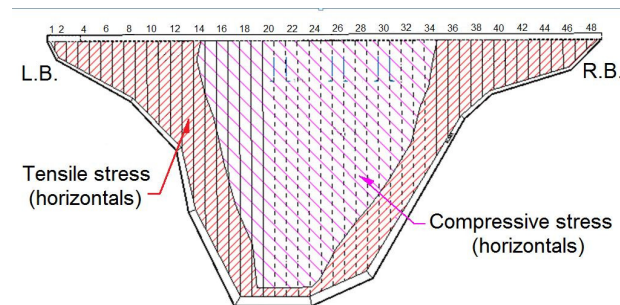


Figure 20. Areas of tension and compression stress in the concrete face.

4 CONCLUSIONS

Geotechnical studies and designs allowed to define the site requirements and use of materials for the dam, as well as to obtain information about the strength and deformability parameters of the alluvium and rockfill used to build the embankment.

The analyses done made possible to establish the importance of using transitions in the zoning of the dam to avoid sudden changes in the modules of deformability of materials that could induce undesirable stress concentrations and lead to tensions and cracking in the concrete face (Marques, 2005; Alberro, 1998).

It was found that the use of very compact gravel-sand in the 3B area will ensure a proper behavior of the concrete face by keeping the maximum displacements in values less than 20 cm, and maximum compression stress at the center concrete face of lower than permissible.

The displacements from 2D analyses are generally two times greater than those obtained in 3D analyses.

Finally, studies and analyses allowed to define the specifications of construction materials to be used in La Yesca dam and are displayed in table 7 and figure 21.

Table 7. Placement and compaction specifications⁴

Zone	Layer Thickness m	Compaction type	Number of passes
1B	0.3	Compacted by dozer	NA
2F	0.3	10.6 Ton VR/ 10 ton NPK plate	6
2 ¹	0.3	10.6 Ton VR/ 10 ton NPK plate	8
3B ²	0.6	12.2 Ton VR	6
T ³	0.8	12.2 Ton VR	6
3C ³	1.0	12.2 Ton VR	6
4	NA	Placed by backhoe	NA

1. The material 2 was designed according to the Sherard criteria (1985). It was also considered useful as filter for 1B and 2F materials.

2. Gravels and sand compacted dry

3. Compaction adding 200 litres of water per m³ of material

4. The specifications also take into account the empiric approach of JB Cooke (1984, 1998 and 2002

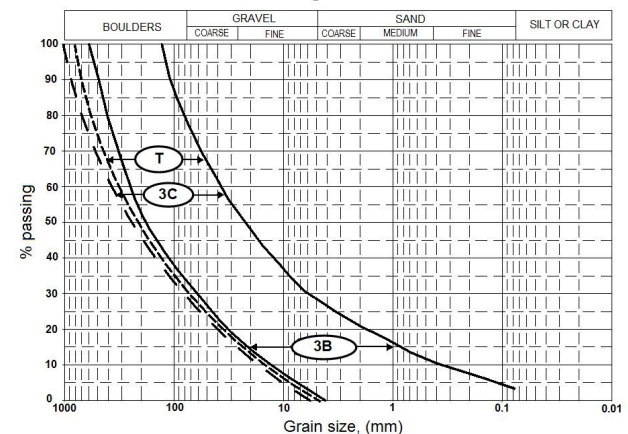


Figure 21. Grain size Band for the curtain specified materials (3B, T, 3C and F)

6. REFERENCES

- Alberro J A. (1998), "Agrietamiento de presas de enrocamiento con cara de concreto", Memorias de la Conferencia Internacional sobre Presas de Almacenamiento, SMMS,
- Aleman JD, et al, 2006, "Studies and geotechnical design of the El Cajon Dam". Proceedings of the International Symposium of Dams, ICOLD-SPANCOLD Barcelona, Spain, Vol. 1
- Aleman JD, et al, 2006, "El Cajon dam, Analysis of its behavior during construction and first filling". Proceedings of 5th International Conference of Dam Engineering, LNAEc, Lisbon, Portugal, 2007
- Cooke J B. (1984), Progress in RockFill Dams, Journal of Geotechnical Engineering, ASCE, october 1984.
- Cooke, J B. (1998), "Empirical Design of CFRD", Hydropower & Dam, Issue six, 1998
- Cooke, J B. (2002), "Report of Dam Visit" of March 4-8, 2002.

- Sherard, J.L. October 1985. "The Upstream Zone in Concrete - Face Rockfill Dams", ASCE Symposium on Concrete Face Rockfill Dams. Detroit, USA.
- Cedro O, et al, 2006, "Características geológicas y estructurales del banco de roca El Pitayo, para el pedraplén de prueba 2, del P. H. La Yesca, Jal. – Nay.", CFE, GEIC, Subgerencia de Exploración Geológica y Geofísica Diciembre de 2006.
- Cedro O, et al, 2006, "Características geológicas y estructurales del banco de roca El Guamúchil, para el pedraplén de prueba 1 del P. H. La Yesca, Jal. – Nay.", CFE, GEIC, Subgerencia de Exploración Geológica y Geofísica, Diciembre de 2006.
- Garrido JL, et al, 2007, 5.2 Obras de contención. Abril 2007. Subgerencia de Estudios Geológicos, GEIC, CFE.
- Vázquez JL, et al, 2004, Informe No. 04-57-SGM/S. "P.H. La Yesca. Estudio preliminar de bancos de materiales. Primera etapa de estudio". Junio de 2004. Subgerencia de Geotecnia y Materiales, GIEC, CFE.
- Vázquez JL, et al, 2006, Informe No. 06-26-SGM/S. "Estudio geotécnico de los bancos de arena limosa y de material impermeable del Ph La Yesca". Subgerencia de Geotecnia y Materiales, GIEC, CFE.
- Pantoja A, et al, 2006, Informe No. 06-32-SGM/S. "P.H. La Yesca. Estudio geotécnico de material granular." Agosto de 2006. Subgerencia de Geotecnia y Materiales, GEIC, CFE.
- Pantoja A, et al, 2006, Informe No. 06-62-SGM/S. "P.H. La Yesca. Informe del pedraplén de aluvión". Diciembre de 2006. Subgerencia de Geotecnia y Materiales, GEIC, CFE.
- Pantoja A, et al, 2007, Informe No. 07-05-SGM/S. "P.H. La Yesca. Informe de los pedraplenes de enrocamiento". Marzo de 2006. Subgerencia de Geotecnia y Materiales, GEIC, CFE.
- Pantoja A, et al, 2007, Informe No. 07-09-SGM/S. "P.H. La Yesca. Análisis y Diseño Gotécnico de la Ataguías". Mayo de 2006. Subgerencia de Geotecnia y Materiales, GEIC, CFE.
- Marsal R J., 1972, "Resistencia y deformabilidad de enrocamientos y gravas", Informe No. 306, Instituto de Ingeniería, UNAM, Mexico
- Alberro J, Gaziev E, 2000, "Resistencia y compresibilidad de los enrocamientos", Instituto de Ingeniería, UNAM.
- Montañez L, Hacelas J. y Castro J. Design of Aguamilpa Dam,
- Sixto Fernández R. y Marco Delgado V. Estudio de Peligro Sísmico, P.H. La Yesca, Nayarit., Departamento de Sismotectónica, GEIC, CFE. Julio 2006.
- Hacelas J E, (1998), Evolution in design and construction of the concrete face rockfill dam, Conferencia internacional sobre presas de almacenamiento, México, julio de 1998, SMMS
- Itasca Consulting Group, Inc. Minnesota, USA, 2002. Fast Lagrangian Análisis of Continua in 3 Dimensions (FLAC3D).
- Stanley D. Wilson and Raul J. Marsal, 1976. "Current trends in design and construction of embankment dams".
- Resendiz J, et al, 2004, Informe No. 04-42-SGM/M. "P.H. La Yesca. Estudio de bancos de materiales", CFE México